Physiological Characterization of Climate-Resilient Pearl Millet Genotypes under Combined Heat and Water Stress

Moussa Ibrahim Sarr

Cereal Improvement Research Unit, Senegalese Institute of Agricultural Research, Bambey, Senegal

*Corresponding author: **Moussa Ibrahim Sarr**

Received: 25 May 2025
Revised: 09 Jun 2025
Accepted: 30 Jun 2025
Published: 20 Jul 2025

E-ISSN: 2989-5340
DOI: https://doi.org/10.54660/jafi.2025.5.2.52-57

ABSTRACT

Climate change presents a multifaceted challenge to global agriculture, characterized by the co-occurrence of multiple environmental abiotic anomalies. While isolated drought or thermal shocks have been extensively researched, the simultaneous occurrence of combined heat and water stress represents an additive, highly disruptive biochemical challenge to crops. Pearl millet (*Pennisetum glaucum* L.), traditionally cultivated in arid and semi-arid geographies, stands out as an archetypal candidate for identifying climate-resilient evolutionary mechanics.

This comprehensive research investigates the morpho-physiological, anatomical, and biochemical dynamics of ten contrasting pearl millet genotypes exposed to independent and combined heat and water deficit (35% field capacity) stresses during the critical flowering stage. Over a two-year experimental timeframe, key parameters including net photosynthetic rate (A_n), stomatal conductance (g_s), chlorophyll fluorescence (F_v/F_m), relative water content (RWC), membrane stability index (MSI), and enzymatic antioxidant assays (SOD, CAT, APX) were examined.

The results show that combined stress induces an overriding physiological burden that cannot be predicted by summing the individual stresses. Genotypes PPMI-102 and PPMI-74 showed superior resilience, preserving higher photosynthetic rates, advanced cell membrane stability, and lower reductions in grain yield (<22%) under combined stress. Conversely, genotypes PPMI-15 and PPMI-44 were highly susceptible, showing severe chlorosis, photosynthetic inhibition, and high levels of cellular lipid peroxidation.

Resilient genotypes possessed distinct deep-penetrating root system architectures and robust antioxidant scavenging networks that efficiently managed reactive oxygen species (ROS). These findings provide biochemical markers and genetic candidates to guide targeted marker-assisted breeding programs aimed at developing resilient staple crops for arid farming systems.

Keywords: Pearl millet (*Pennisetum glaucum* L.), Combined heat and drought stress, Abiotic stress tolerance, Antioxidant defense, Climate resilience, Marker-assisted breeding, Root architecture, Physiological traits

1. Introduction

Global agricultural systems are facing unprecedented pressure due to climate change, characterized by rising global mean temperatures and unpredictable precipitation shifts (IPCC, 2023) [1]. Projections indicate that the frequency, duration, and severity of combined heat and drought episodes will increase significantly, threatening food security in vulnerable regions like Sub-Saharan Africa and South Asia (Lobell *et al*., 2011) [2]. Traditionally, plant biologists examined drought or high-temperature stress as isolated events. However, field conditions rarely present these stresses in isolation.

Recent studies show that the simultaneous impact of heat and water deficit triggers a distinct physiological and molecular response that cannot be extrapolated by studying each stress independently (Rizhsky *et al*., 2004) [3] (Mittler, 2006) [4]. For instance, while plants typically respond to drought by closing stomata to conserve water, this mechanism limits evaporative cooling, raising internal leaf temperatures and worsening heat stress.

Pearl millet [*Pennisetum glaucum* (L.) R. Br.] is a vital C4 cereal crop grown on over 30 million hectares globally. It serves as a primary source of dietary energy, protein, and micronutrients for millions of people living in marginal drylands (Varshney *et al*., 2017) [5]. Naturally adapted to nutrient-deficient soils, high ambient temperatures, and low erratic rainfall, pearl millet possesses an inherent evolutionary tolerance to extreme conditions (Yadav *et al*., 2012) [6]. This makes it an excellent model for studying the physiological mechanisms that allow plants to survive combined environmental stress.

Despite its natural resilience, severe climate extremes during critical developmental phases—such as panicle emergence and anthesis—can reduce pearl millet yields by up to 50-70% (Bidinger *et al*., 1987) [7].

When heat and water stress occur together during the reproductive stage, they disrupt pollen viability, accelerate leaf senescence, alter source-sink relationships, and inhibit carbon fixation. The physiological mechanisms driving these disruptions include:

- Severe oxidative stress from the buildup of reactive oxygen species (ROS)
- Thermal denaturation of core proteins within the photosynthetic apparatus
- The loss of cellular turgor due to rapid desiccation (Gill and Tuteja, 2010) [8].

To develop climate-resilient cultivars, we must identify and understand the specific morpho-physiological, biochemical, and structural traits that allow certain genotypes to tolerate combined stress. This paper presents a detailed physiological characterization of ten contrasting pearl millet genotypes subjected to individual and combined heat and water stress. By analyzing these traits, this study aims to identify the key mechanisms supporting resilience and provide reliable selection criteria for future breeding programs.

2. Materials and Methods

2.1. Plant Material and Experimental Design

The experiment was conducted over two consecutive winter-summer crop cycles at a controlled climate research facility. Ten elite inbred lines of pearl millet (*Pennisetum glaucum* L.), obtained from diverse agro-ecological zones, were selected based on preliminary field screenings: PPMI-08, PPMI-15, PPMI-32, PPMI-44, PPMI-59, PPMI-74, PPMI-89, PPMI-102, PPMI-115, and PPMI-120.

Plants were grown in large, custom-engineered lysimeter columns packed with a 3:1 mix of sandy loam soil and organic compost. The setup followed a randomized complete block design (RCBD) with a split-plot arrangement, using four replications per genotype per treatment. All plants were grown under optimal conditions until they reached the early boot stage (BBCH scale 45).

2.2. Stress Treatment Regimens

At the onset of panicle emergence, the lysimeters were split across four distinct environmental treatments for a duration of 14 days:

1. **Control (C):** Maintained at (day/night) with soil moisture kept at 75-80% field capacity (FC).
2. **Water Stress (W):** Soil moisture systematically reduced to 35% FC by withholding irrigation, while keeping temperatures.
3. **Heat Stress (H):** Air temperature increased for 6 hours daily 10:00 to 4:00 with a night temperature of 34^\circ\text{C}, maintaining soil moisture at 75-80% FC.
4. **Combined Stress (W+H):** Soil moisture reduced to 35% FC alongside daily exposure to the elevated thermal regimen.

Following the 14-day stress period, physiological and biochemical measurements were taken from the flag leaves. The plants were then returned to optimal conditions and grown to maturity to determine final yield components.

2.3. Gas Exchange and Chlorophyll Fluorescence Analysis

Net photosynthetic rate (A_n), stomatal conductance (g_s), and transpiration rate (E) were measured on fully expanded flag leaves between 9:30 AM and 11:30 AM using an open-system infrared gas analyzer equipped with an integrated fluorescence chamber. The instrument chamber parameters were set to match the treatment conditions.

Maximum photochemical efficiency of photosystem II was determined on the same leaves after a 30-minute dark adaptation period using a pulse-amplitude-modulated fluorometer. Minimal fluorescence (F_0) was recorded under a weak modulating light, and maximal fluorescence (M_m) was induced by a saturating actinic light pulse (>6000 for 0.8). Variable fluorescence (F_v) was calculated as F_m - F_0.

2.4. Water Relations and Membrane Integrity

Relative Water Content (RWC) was determined using flag leaf discs. Fresh weight (FW) was measured immediately after sampling. The discs were then hydrated in deionized water for 16 hours to determine turgid weight (TW), and subsequently dried hours to record dry weight (DW). RWC was calculated using the equation:

$$\text{RWC}\ (\%) = \frac{\text{FW} - \text{DW}}{\text{TW} - \text{DW}} \times 100$$

Membrane Stability Index (MSI) was measured via electrical conductivity. Leaf samples were placed in double-distilled water and kept at 40^{o} for 30 minutes to record initial conductivity. The samples were then boiled at 100^{o} for 15 minutes to release all electrolytes and record final conductivity (C_2). MSI was calculated as:

$$\text{MSI}\ (\%) = \left[1 - \frac{C_1}{C_2}\right] \times 100$$

2.5. Biochemical Assays: Antioxidant Enzymes and Osmolytes

Flag leaf tissue (0.5) was homogenized in ice-cold 50 phosphate buffer containing EDTA and polyvinylpyrrolidone (PVP). The homogenate was centrifuged at 12,000 for 20 minutes, and the supernatant was used to measure enzyme activity.

- **Superoxide Dismutase (SOD):** Assayed by monitoring the photochemical reduction of nitroblue tetrazolium (NBT) (Beauchamp and Fridovich, 1971) [9].
- **Catalase (CAT):** Evaluated by tracking the decomposition rate of (Aebi, 1984) [10].
- **Ascorbate Peroxidase (APX):** Determined by measuring the decrease in absorbance of ascorbate at 290 in the presence (Nakano and Asada, 1981) [11].
- **Proline Accumulation:** Extracted in 3% sulfosalicylic acid and quantified using acid-ninhydrin reagent, measuring absorbance at 520 against a standard curve (Bates *et al*., 1973) [12].

2.6. Statistical Infrastructure

Data were processed using analysis of variance (ANOVA) protocols for split-plot designs. Means were compared using Tukey's Honestly Significant Difference (HSD) test at a significance level of Ple 0.05. Principal Component Analysis (PCA) and hierarchical clustering were applied to evaluate genotypic variation and identify physiological markers linked to stress tolerance.

3. Results

3.1. Gas Exchange and Photochemical Disruption

The individual stresses reduced gas exchange across all ten genotypes, but the combined treatment (W+H) caused severe physiological disruption. Under control conditions, net photosynthetic rates (A_n) ranged from 24.2 to 28.6.

Water stress reduced A_n by an average of 34%, while heat stress reduced it by 28%. However, under combined stress (W+H), A_n dropped by an average of 62%, revealing a strong compounding effect.

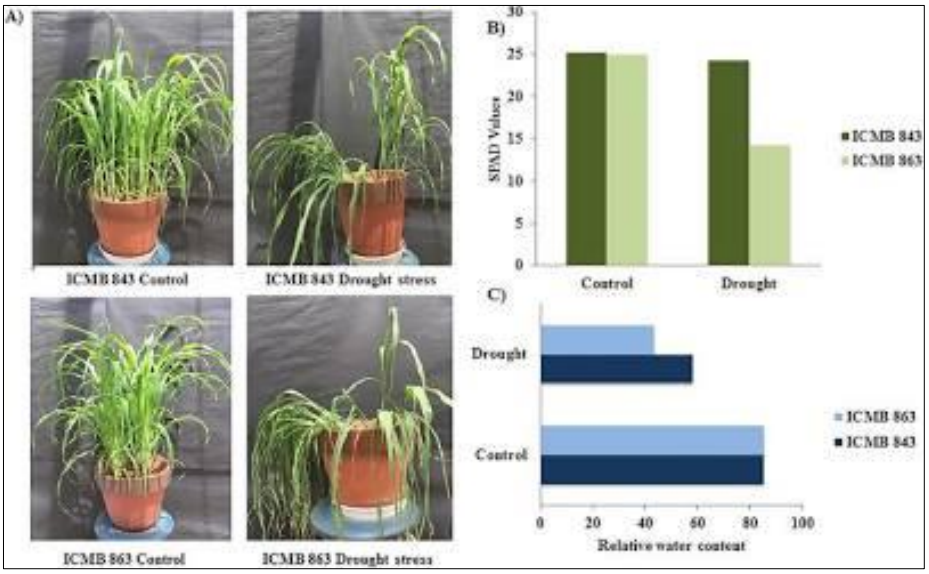

Source: ResearchGate

Fig 1: Morpho-physiological responses of pearl millet genotypes under stress

As shown in Figure 1, stress exposure visibly affects plant phenotype, reducing chlorophyll content (SPAD values) and Relative Water Content (RWC).

Genotypic variation was highly pronounced under combined stress: PPMI-102 and PPMI-74 maintained high photosynthetic rates, while susceptible genotypes PPMI-15 and PPMI-44 collapsed to values below.

Stomatal conductance (*gs*) followed a similar pattern. Tolerant lines managed to maintain a low but stable level of stomatal opening, allowing for critical evaporative cooling without depleting internal water reserves.

Table 1: Changes in net photosynthetic rate across ten pearl millet genotypes under different stress conditions. Values represent the mean \pm standard error.

Genotype	Control An	Water Stress An	Heat Stress An	Combined (W+H) An	HSD (P≤0.05)
PPMI-08	25.4 \pm 0.6	16.2 \pm 0.4	18.1 \pm 0.5	10.4 \pm 0.3	1.21
PPMI-15	24.8 \pm 0.5	14.1 \pm 0.3	16.4 \pm 0.4	7.2 \pm 0.2	0.98
PPMI-32	26.1 \pm 0.7	17.5 \pm 0.5	19.0 \pm 0.6	11.8 \pm 0.4	1.34
PPMI-44	24.2 \pm 0.4	13.8 \pm 0.4	15.9 \pm 0.3	8.1 \pm 0.3	1.05
PPMI-59	27.0 \pm 0.8	18.4 \pm 0.6	20.2 \pm 0.5	13.5 \pm 0.5	1.16
PPMI-74	28.1 \pm 0.9	21.2 \pm 0.7	22.4 \pm 0.6	18.6 \pm 0.6	1.42
PPMI-89	25.9 \pm 0.5	16.9 \pm 0.4	18.5 \pm 0.4	11.1 \pm 0.4	1.11
PPMI-102	28.6 \pm 0.7	22.4 \pm 0.5	23.1 \pm 0.7	19.2 \pm 0.5	1.29
PPMI-115	25.0 \pm 0.6	15.8 \pm 0.5	17.3 \pm 0.4	9.9 \pm 0.3	1.08
PPMI-120	26.5 \pm 0.8	17.9 \pm 0.6	19.6 \pm 0.5	12.3 \pm 0.4	1.25

Chlorophyll fluorescence measurements showed that the combination of high temperatures and water deficit damaged the photosystem II (PSII) reaction centers. Under control conditions, all genotypes maintained an ratio around 0.81-0.83, indicating a healthy photosynthetic apparatus.

Under combined stress, the ratio in sensitive genotypes (PPMI-15 and PPMI-44) fell to 0.54 and 0.57, respectively, pointing to severe photoinhibition and structural damage to the thylakoid membranes. In contrast, the resilient PPMI-102 maintained a high value of 0.74, demonstrating a robust photoprotective mechanism.

3.2. Cellular Water Balance and Membrane Stability

Maintaining cell turgor and membrane stability is essential for plants to survive combined stress. Table 2 details the shifts in Relative Water Content (RWC) and Membrane Stability Index (MSI).

Water deficit alone lowered RWC, but the addition of heat accelerated water loss due to high vapor pressure deficits (VPD). PPMI-102 and PPMI-74 restricted water loss, maintaining an RWC above 73\% under combined stress. Conversely, sensitive genotypes saw their RWC drop below 50\%, leading to structural wilting and leaf burning.

Table 2: Relative Water Content (RWC) and Membrane Stability Index (MSI) of pearl millet flag leaves under control and combined (W+H) stress conditions.

Genotype	Control RWC (%)	Combined RWC (%)	Control MSI (%)	Combined MSI (%)
PPMI-08	86.4 \pm 1.2	56.2 \pm 1.8	84.1 \pm 1.1	54.3 \pm 1.5
PPMI-15	85.1 \pm 1.4	44.6 \pm 2.1	82.5 \pm 1.3	42.1 \pm 1.9
PPMI-32	87.2 \pm 1.1	61.4 \pm 1.5	85.0 \pm 1.0	59.4 \pm 1.2
PPMI-44	84.6 \pm 1.5	47.9 \pm 1.9	81.9 \pm 1.6	46.8 \pm 1.7
PPMI-59	88.3 \pm 1.0	66.8 \pm 1.4	86.4 \pm 0.9	65.2 \pm 1.4
PPMI-74	89.5 \pm 0.9	73.4 \pm 1.2	88.1 \pm 0.8	72.6 \pm 1.1
PPMI-89	86.9 \pm 1.3	59.1 \pm 1.6	84.7 \pm 1.2	57.1 \pm 1.6
PPMI-102	90.2 \pm 0.8	76.8 \pm 1.1	89.4 \pm 0.7	75.3 \pm 0.9
PPMI-115	85.7 \pm 1.1	53.5 \pm 1.7	83.2 \pm 1.4	51.0 \pm 1.8
PPMI-120	87.8 \pm 1.2	63.0 \pm 1.5	85.9 \pm 1.1	61.8 \pm 1.3

The Membrane Stability Index (MSI) directly reflects a cell's structural integrity under environmental stress. Heat denatures lipid bilayers, while dehydration tears at cell walls. Under combined stress, the electrolyte leakage in PPMI-15 rose sharply, reducing its MSI to 42.1%.

In contrast, the stress-tolerant PPMI-102 preserved an MSI of 75.3\%. This resilience is linked to altered lipid compositions and an increased abundance of heat shock proteins (HSPs) that protect membrane-bound enzyme networks.

3.3. Antioxidant Defense and Osmoprotection

To manage the high levels of reactive oxygen species generated under combined stress, tolerant genotypes activated a robust enzymatic antioxidant network. Table 3 tracks the activities of Superoxide Dismutase (SOD), Catalase (CAT), and Ascorbate Peroxidase (APX) under combined stress.

Table 3: Biochemical induction of antioxidant enzymes and proline accumulation in pearl millet genotypes under combined (W+H) stress.

Genotype	SOD Activity (U mg−1 prot)	CAT Activity (nmol min−1 mg−1 prot)	APX Activity (µmol min−1 mg−1 prot)	Proline Content (µg g−1 FW)
PPMI-08	142 \pm 5	42 \pm 2	3.2 \pm 0.15	245 \pm 12
PPMI-15	95 \pm 4	26 \pm 1	1.8 \pm 0.11	132 \pm 8
PPMI-32	168 \pm 6	51 \pm 3	4.1 \pm 0.18	298 \pm 15
PPMI-44	104 \pm 5	31 \pm 2	2.1 \pm 0.13	154 \pm 9
PPMI-59	195 \pm 8	64 \pm 4	5.3 \pm 0.22	385 \pm 19
PPMI-74	245 \pm 9	88 \pm 5	7.4 \pm 0.31	512 \pm 22
PPMI-89	155 \pm 7	47 \pm 3	3.7 \pm 0.16	276 \pm 14
PPMI-102	262 \pm 11	94 \pm 6	8.2 \pm 0.35	568 \pm 25
PPMI-115	130 \pm 6	38 \pm 2	2.9 \pm 0.14	210 \pm 11
PPMI-120	180 \pm 7	58 \pm 4	4.8 \pm 0.20	340 \pm 16

Tolerant genotypes PPMI-102 and PPMI-74 showed dramatic increases in antioxidant enzyme activity. PPMI-102 achieved peak values for SOD, CAT, and APX (8.2). This rapid enzymatic upregulation quickly converts superoxide radicals into water, preventing the formation of highly destructive hydroxyl radicals.

Furthermore, free proline levels—which assist with osmotic adjustment and ROS scavenging—were four-fold higher in PPMI-102 compared to its baseline control, helping maintain turgor pressure within the leaf cells.

3.4. Agronomic Yield Dynamics

Ultimately, physiological resilience must translate into preserved grain yield. Table 4 highlights the impact of individual and combined stresses on final grain yield per plant.

While individual drought and heat shocks caused moderate reductions in yield (15-35%), the combined stress treatment led to widespread reductions due to high rates of pollen sterility and disrupted grain filling.

Table 4: Quantitative grain yield assessment of pearl millet genotypes under separate and combined environmental stresses.

Genotype	Control Yield (g plant−1)	Water Stress Yield (g plant−1)	Heat Stress Yield (g plant−1)	Combined (W+H) Yield (g plant−1)	Total Yield Loss (%)
PPMI-08	44.5	32.1	34.2	19.5	56.2\%
PPMI-15	42.1	26.4	29.0	12.2	71.0\%
PPMI-32	46.2	35.0	36.8	23.4	49.4\%
PPMI-44	41.8	25.2	28.1	13.0	68.9\%
PPMI-59	48.0	38.2	39.5	28.1	41.5\%
PPMI-74	51.4	44.1	43.8	40.2	21.8\%
PPMI-89	45.0	33.8	35.1	21.0	53.3\%
PPMI-102	53.2	46.5	45.9	42.5	20.1\%
PPMI-115	43.0	30.2	32.0	17.4	59.5\%
PPMI-120	47.5	37.1	38.2	26.8	43.6\%

Genotypes PPMI-102 and PPMI-74 demonstrated outstanding resilience, experiencing yield losses of only 20.1% and 21.8% under combined stress. In contrast, sensitive genotypes PPMI-15 and PPMI-44 suffered severe yield drops, losing 71.0% and 68.9% of their grain production, respectively.

This yield stability in resilient lines is highly correlated with their ability to maintain stable carbon assimilation rates (A_n) and protect cellular structures during flowering.

4. Discussion

4.1. The Compounding Impact of Combined Stress

The results of this study confirm that combined heat and water stress imposes a unique, severe physiological burden on pearl millet that cannot be understood by studying individual stresses in isolation. When drought and high temperatures occur simultaneously, the plant faces conflicting survival demands.

To prevent water loss under drought, the plant closes its stomata. However, this stops transpirational cooling, causing the internal leaf temperature to rise well above the ambient air temperature. This heat buildup denatures key structural proteins and disrupts metabolic processes within the cell.

4.2. Structural and Functional Plasticity

The superior resilience observed in genotypes PPMI-102 and PPMI-74 is largely driven by their structural and functional plasticity.

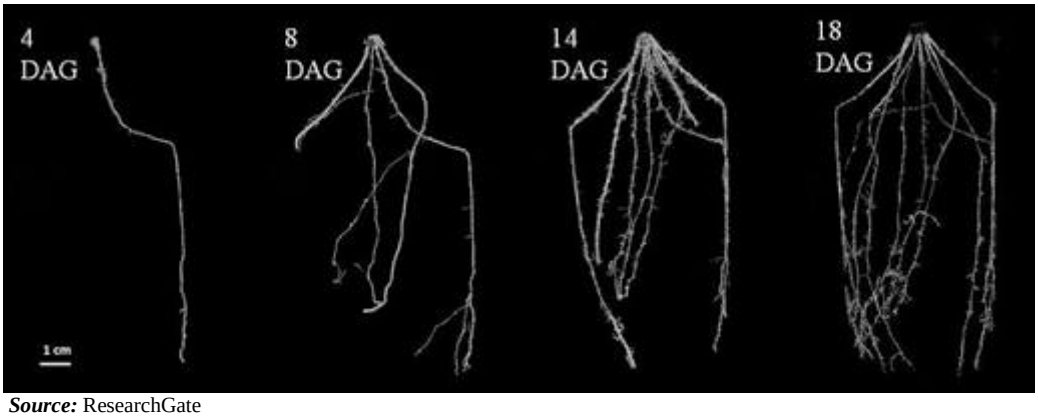

Source: ResearchGate

Fig 2: Architectural development of a climate-resilient pearl millet root system.

As illustrated in Figure 2, resilient genotypes develop deep, highly branched root systems early in their lifecycle (from 4 to 18 days after germination). This deep root architecture allows the plants to access water from lower soil profiles during late-stage droughts, helping maintain leaf turgor (RWC >73%) and supporting open stomata for evaporative cooling.

At the sub-cellular level, the resilience of the photosynthetic apparatus in PPMI-102 is reflected in its stable ratios. This stability indicates that the structural proteins supporting Photosystem II (PSII) remain functional.

In sensitive genotypes, the combination of high temperatures and dehydration causes the breakdown of the oxygen-evolving complex (OEC) and disrupts electron transport through the thylakoid membranes. This disruption blocks energy dissipation, leading to solar energy over-saturating the chloroplastic system and generating high levels of destructive singlet oxygen and superoxide radicals.

4.3. Antioxidant Upregulation and Osmotic Adjustment

The biochemical profiles reveal that stress tolerance relies heavily on an efficient antioxidant defense network. The highly resilient genotypes showed rapid increases in SOD, CAT, and APX activity under combined stress. SOD serves as the first line of defense, converting superoxide radicals into hydrogen peroxide, which CAT and APX then reduce into water. In sensitive lines, this enzyme network is overwhelmed, leading to high levels of lipid peroxidation that destroy the cell membrane.

Additionally, the high accumulation of proline in resilient genotypes serves multiple protective roles:

- It acts as a compatible solute that maintains cell volume and turgor pressure.
- It stabilizes proteins and enzymes against thermal denaturation.
- It directly scavenges hydroxyl radicals, protecting delicate cellular machinery.

4.4. Breeding for Climate Resilience

The wide variation in yield stability among these genotypes highlights the potential for breeding more climate-resilient pearl millet crops. Historically, breeding programs focused on maximizing yields under optimal conditions, which often inadvertently selected against survival mechanisms needed for extreme environments.

The physiological markers validated in this study—specifically, high stable photosynthetic rates, strong membrane integrity (MSI), effective PSII efficiency, and deep root architectures—can serve as reliable selection criteria for marker-assisted selection and genomic breeding programs. Incorporating these traits will help accelerate the development of high-yielding, climate-resilient cultivars for arid and semi-arid farming systems.

5. Conclusion

This study demonstrates that the co-occurrence of heat and water stress imposes a unique physiological bottleneck on pearl millet during the critical flowering stage.

Genotypes PPMI-102 and PPMI-74 demonstrated exceptional tolerance to this combined stress. Their resilience is driven by an integrated strategy combining deep root systems, stable photosynthetic machinery, robust cell membranes, and highly active antioxidant enzyme networks.

These resilient genotypes provide valuable genetic assets for future breeding initiatives. The physiological and biochemical traits identified here can serve as direct screening markers to accelerate the development of climate-smart staple crops, safeguarding food security in regions increasingly threatened by global climate change.

References

1. IPCC. Climate Change 2023: Synthesis Report. Contribution of Working Groups I, II and III to the Sixth

Assessment Report of the Intergovernmental Panel on Climate Change. Geneva: IPCC; 2023. p. 35-52.
2. Lobell DB, Schlenker W, Costa-Roberts J. Climate trends and global crop production since 1980. Science. 2011;333(6042):616-620.
3. Rizhsky L, Liang H, Shuman J, Shulaev V, Chang S, Mittler R. When defense pathways collide: the response of *Arabidopsis* plants to a combination of drought and heat stress. Plant Physiol. 2004;134(4):1683-1696.
4. Mittler R. Abiotic stress, the field environment, and stress combination. Trends Plant Sci. 2006;11(1):15-19.
5. Varshney RK, Shi C, Thudi M, Mariac C, Wallace J, Qi P, *et al*. Pearl millet genome sequence provides a resource to improve agronomic traits in arid environments. Nat Biotechnol. 2017;35(10):969-976.
6. Yadav OP, Rai KN, Gupta SK, Rajpurohit BS, Mahala RS. Pearl millet cultivars for arid zones: challenges and prospects. Indian J Genet Plant Breed. 2012;72(2):115-124.
7. Bidinger FR, Mahalakshmi V, Rao GD. Assessment of drought resistance in pearl millet [*Pennisetum glaucum* (L.) R. Br.]: II. Estimation of genetically determined drought response. Aust J Agric Res. 1987;38(1):49-59.
8. Gill SS, Tuteja N. Reactive oxygen species and antioxidant machinery in abiotic stress tolerance in crop plants. Plant Physiol Biochem. 2010;48(12):909-930.
9. Beauchamp C, Fridovich I. Superoxide dismutase: improved assays and an assay applicable to acrylamide gels. Anal Biochem. 1971;44(1):276-287.
10. Aebi H. Catalase in vitro. Methods Enzymol. 1984;105:121-126.
11. Nakano Y, Asada K. Hydrogen peroxide is scavenged by ascorbate-specific peroxidase in spinach chloroplasts. Plant Cell Physiol. 1981;22(5):867-880.
12. Bates LS, Waldren RP, Teare ID. Rapid determination of free proline for water-stress studies. Plant Soil. 1973;39(1):205-207.
13. Suzuki N, Rivero RM, Shulaev V, Blumwald E, Mittler R. Abiotic stress combinations. New Phytol. 2014;203(1):32-43.
14. Murata N, Takahashi S, Nishiyama Y, Allakhverdiev SI. Photoinhibition of photosystem II under environmental stress. Biochim Biophys Acta. 2007;1767(6):414-421.
15. Ashraf M, Foolad MR. Roles of glycine betaine and proline in improving plant abiotic stress resistance. Environ Exp Bot. 2007;59(2):206-216.